22p.

Technical Memorandum No. 33-85

Radio and Optical Space Communications

P. D. Potter

R. Stevens

W. H. Wells

jpl

JET PROPULSION LABORATORY

CALIFORNIA INSTITUTE OF TECHNOLOGY

PASADENA, CALIFORNIA

October 30, 1962

Well 1

NATIONAL AERONAUTICS AND SPACE ADMINISTRATION
CONTRACT NO. NAS 7-100

Technical Memorandum No. 33-85

Radio and Optical Space Communications

P. D. Potter
R. Stevens
W. H. Wells

JET PROPULSION LABORATORY
CALIFORNIA INSTITUTE OF TECHNOLOGY
PASADENA, CALIFORNIA

October 30, 1962

PREFACE

This paper was presented at the Sixth Meeting of the AGARD Avionics Panel, Paris, France, July 6–12, 1962.

CONTENTS

TABLES

FIGURES

ABSTRACT

17336

Coherent electromagnetic energy has been used for many years at radio frequencies for communications and radar, more recently over extremely long distances in space. The invention of a high-coherency light source has produced a quantum jump in the technology of communication systems at optical frequencies. In this Report the theory and state of the art of laser sources is reviewed, with the possible application of these devices to space communications and long-range radar (or lidar). Sample optical and radio-frequency systems are analyzed in detail. Practical system and component problems which arise in optical communication and lidar systems are discussed.

I. INTRODUCTION

Man has been communicating at light frequencies with some objects in space for a good many years, although on a strictly one-way basis. We refer to astronomical observations of stars and other luminous sources and the bistatic radar observations of planets using the Sun as an illuminator. A sizeable amount of very important information has been collected in that way. Thirty years ago observations of astronomical sources were extended to the radio range of frequencies (Jansky), and sixteen years ago an extraterrestrial object (the Moon) was brought under observation by radio-frequency radar techniques using an Earth-based illuminator (U. S. Signal Corps, DeWitt and Stodola; Z. Borg, Hungary). The principal objective of all of the space communications has been to increase man's knowledge of the Universe. Recently, beginning in 1958, a new experimental technique of space exploration by rocket-propelled vehicle has been added (*Sputnik*, et al.), which promises to be very useful, at least throughout the solar system. As with previous techniques, communication plays an essential role in the space vehicle method of exploration. To date, communication with space vehicles has been provided almost entirely by radio-frequency devices, and quite satisfactorily, too.

Recently, the invention of a high-coherency light source (predicted by Schawlow and Townes, 1958, first demonstrated experimentally by Maiman, 1960), has produced a quantum jump in the technology of communication systems at optical frequencies. As a result of that invention, interest in the use of light in its traditional role of providing space communication has also taken a (high-energy) quantum jump. The purpose of this paper is to discuss the probable role of light frequencies in providing communications for space exploration by spacecraft in the next several years. We will also discuss lunar and planetary radar/lidar.

The use of Earth-based radar to explore heavenly bodies (apparently limited to the Sun and near-Earth planets) is related to spacecraft communications for a number of reasons. The results of radar measurements help to define the orbital and physical characteristics of the Moon or planets and some of the conditions of communicating between them and Earth—information which is very useful to a spacecraft designer. The ground-station equipment of a lunar/planetary radar observatory bears a remarkable resemblance to the equipment needed for effective spacecraft radio communications (for example, the 1961 Venus radar experiments performed by the Jet Propulsion Laboratory used the basic antenna, transmitter, receiving, and data handling equipment of the NASA/JPL Goldstone Deep Space Instrumentation Facility).

Because the advent of the new high-coherency light source (the laser) is the real impetus for this paper, we shall begin with a discussion of its characteristics and some of the equipment which would be used with it.

II. COHERENT LIGHT

A. Lasers in General

Most of the technical world has heard about optical masers (lasers) by now. Nevertheless, it seems as though the news is many decades late. All the ingredients for laser research have been available for a long time, namely: spectroscopy, fluorescence studies, and precision interferometry. It is merely an oversight that no one thought of the right combination—a special fluorescence inside an interferometer. In fact, the oversight was not corrected until after the analogous work had been done at microwave frequencies, a part of the spectrum which has been studied only relatively recently.

The purpose of a laser is to generate or amplify a coherent light wave. In these functions, it is the optical analog of a good quality radio-frequency oscillator or amplifier. By comparison to the laser oscillator, all other light sources are noise generators.

The active ingredient in a laser is a substance whose atoms, molecules, or ions have energy levels and transition rates which meet certain requirements. Figure 1 is the energy level diagram of a fictitious substance that may be regarded as ideal for laser action. To activate the material, bright light of high frequency, typically green to ultraviolet, is shone on the material, pumping it into the band of higher energy levels. Other means of excitation may be substituted for light. The transitions induced by pumping excitation are reversible, as indicated by the two-headed arrows in Fig. 1, but nevertheless, pumping results in a considerable average population of the high levels which otherwise would be virtually unpopulated. Many of the excited levels relax, either by spontaneous emission, or some radiationless mechanism, to the lower level labeled (2). Radiation of a photon further relaxes to level (1), and a final relaxation returns the atomic system to its ground state. The net result is conversion of high-frequency light, f_p, to the lower frequency,

$$f_M = (E_2 - E_1)/h$$

So far, this is merely a description of fluorescence, like the brilliant glow of certain minerals when illuminated with "black light" from an ultraviolet lamp, except that the emission is required to be narrow band, while the absorption is preferably wide band.

A further requirement for laser action is that the relaxation rates satisfy certain relations. The essence of these

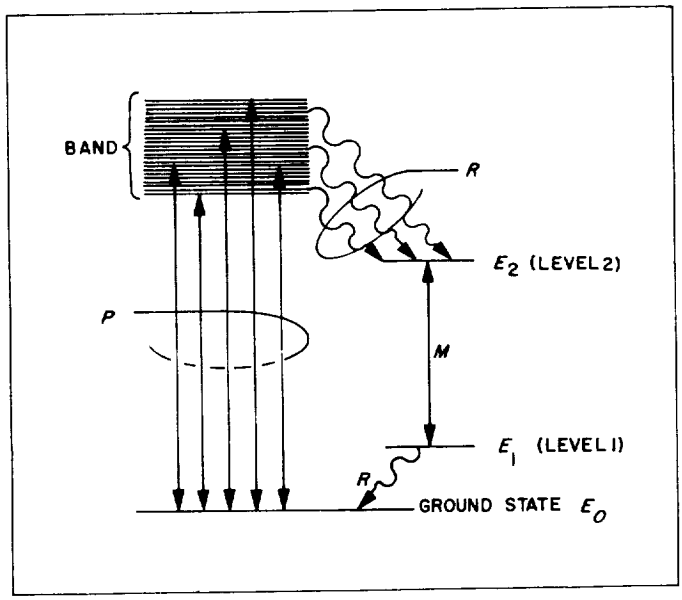

Fig. 1. Energy level diagram

relations is that the rate from level (2) to (1) be relatively slow, so that this transition serves as a bottleneck. This condition results in the mean population of (2) being greater than (1), i.e., the relative populations are "inverted" from the ordinary thermal condition in which the lower state always has the greater population. The inverted population of two levels is the essence of maser action, and is the only purpose served by the scheme of pumping and relaxation described. Any other valid scheme for inverting populations may be substituted, so the ideal energy levels are not to be taken too seriously. Laser energy level schemes to date bear only remote resemblance to Fig. 1.

Now consider what happens when radiation at the frequency, f_M, strikes the active substance. Normally, one would expect the radiation to be absorbed, but because of the inverted populations, the stimulated emission from the upper level more than compensates the absorption. The result is that the radiation is amplified as it passes through the substance. That is, the absorption coefficient is negative, and the wave grows exponentially (to a saturation point) instead of decaying exponentially as in the normal case.

An amplifying material may be converted into an oscillator by closing a feedback loop from the output back to the input. Optically this is done by enclosing the active

material between reflecting end plates, since there is no distinction between the input and output sides of the material. This is shown in Fig. 2. One mirror is partially (e.g., 5%) transmitting to allow the output to escape. The sum of right and left running waves in the resonator is a standing wave, or high-order mode. The mirrors may be plane, or slightly concave. The latter squeezes the standing wave pattern toward the axis and helps reduce diffraction losses. One popular configuration is confocal mirrors (Refs. 1 and 2). This means that the focal points of the mirrors coincide, or the center of curvature of each falls on the surface of the other.

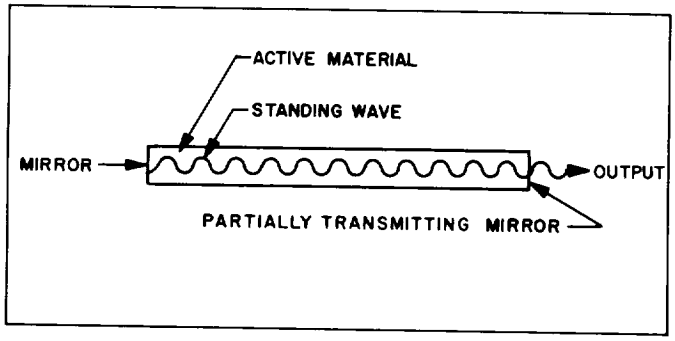

Fig. 2. Optical cavity, or Fabry-Perot interferometer

Let us contrast the properties of an optical resonator to those of a microwave cavity. At microwave frequencies, the modes of a resonant cavity are widely spaced compared to the sharpness of a molecular[1] resonance. Therefore, a maser must be tuned to bring the cavity resonance into coincidence with a molecular resonance. When this is achieved, the maser operating frequency is determined primarily by the molecular resonance, its bandwidth being much sharper than the response of the cavity, as shown in Fig. 3a. The cavity has only a small pulling effect, moving the oscillating frequency a little to one side of the molecular peak. In contrast to this situation, the relation of optical resonators to the molecular resonance is shown in Fig. 3b. The cavity need not be tuned to obtain oscillation, one mode will always fall within the molecular line even if the laser material is chosen to have particularly sharp lines. In this case, the oscillation will occur almost at the peak of the most favored cavity resonance, but pulled slightly by the molecular resonance. Excitation of more than one mode at a time has been demonstrated. Normally this is to be avoided if possible, because it degrades the purity of the generated light.

[1] In this sense, "molecule" serves as a generic term for the active molecules, atoms, or ions.

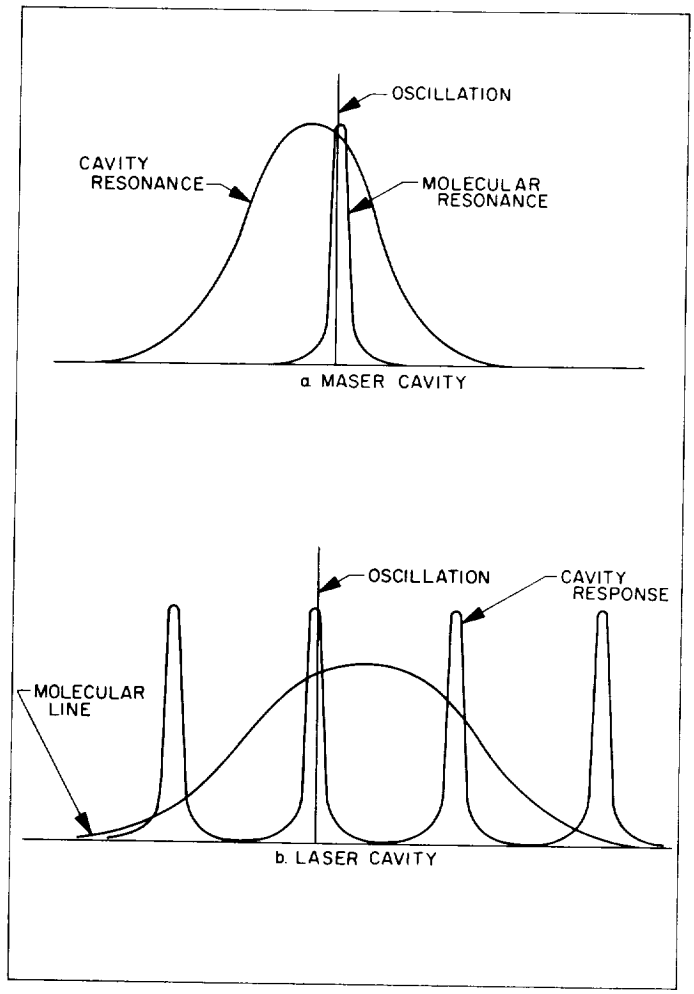

Fig. 3. Maser and laser cavities and molecular responses

For an interferometer of length L, refractive index n, the spacing of resonances in wavelength units is given by

$$\Delta\lambda = \lambda^2/2nL$$

This follows from the fact that there is one mode for each integral number of half wavelengths that may be fitted in the length L. For a typical wavelength of 1 μ this gives

$$\Delta L = (0.5/nL)\ \text{Å}$$

when nL is in centimeters. This is a narrow spacing indeed, considering that nL may be 5 or even 100 cm. Perhaps spacing in frequency units is more meaningful. It is

$$\Delta\nu = c/2nL$$

For example,

$$\Delta\nu = 3 \times 10^9 \text{ cps when } nL = 5 \text{ cm}$$

$$\Delta\nu = 150 \text{ mc when } nL = 100 \text{ cm}$$

Normally laser oscillator design strives to excite a single mode of the cavity. If this goal were realized, the frequency and spacial configuration of the output radiation would be essentially exactly known, i.e., given the intensity and phase of the output wave at any point and at any time, the intensity and phase at any other point and time could be calculated. This is because the radiation would always be at the frequency and in the spacial configuration characteristic of the excited mode.

The degree to which this ideal is approached in its time dependence is a measure of temporal coherence. This is equivalent to spectral purity of the wave. If the wave is a perfect sinusoid (or other periodic function), then knowledge of the phase at one time determines the phase precisely for all subsequent time. But if the wave has bandwidth $\Delta\nu$, then considerable doubt accumulates after a time $\Delta\nu^{-1}$.

Spacial coherence[2] is equivalent to a point source in geometric optics. Of course, it is not really a point, but a volume having dimensions the order of distances over which geometric optics is barely valid, i.e., the order of a wavelength at the color in question. The ideal laser produces that wavefront which is characteristic of a particular mode of the resonator, and, therefore, may in principle be exactly known. This wavefront may be reshaped by focusing elements into a converging spherical front. To as close a dimension as is valid in geometric optics, a converging sphere focuses down to a point.

All light sources prior to the discovery of lasers were sources of (considerable) finite size. Since the phase of light from one part of an extended source is random compared to another part, it is impossible to focus light from such a source to a "point," only the finite-sized images given by the principles of geometric optics can be obtained. With conventional sources, one can approach coherence as nearly as desired by receding to a great distance where the source looks like a point, and by filtering out all but a very narrow band of frequencies. But in this case, coherence is obtained by rejection of all but a tiny fraction of the power. It is much more desirable to have the power generated coherently at the source. By accomplishing this, the laser makes available power fluxes that were previously unheard of. For example, ruby lasers have been reported to operate at power levels approaching 3 Mw peak. If focused in an area of 3 square microns, this gives the astonishing power flux of 10^{18} w/m^2. This corresponds to an electric field of 3×10^7 v/mm! Already a number of novel effects, including two photon transitions (Ref. 3) and overtones of optical frequencies (Ref. 4) have been observed using the new intensity range as a research tool.

[2] For a traveling wave, spacial coherence refers to the spacial dimensions normal to a ray. Coherence along a ray is equivalent to temporal coherence. (Divide distance by c to get time.)

B. Lasers in Particular

Solids. Good candidates for laser materials are small quantities of rare earths and transition elements doped into a host crystal or glass. The peculiar shell structure of these elements permits electronic transitions in the optical band that are not greatly disturbed by the surrounding host material. The transparent host material spaces the active sites to prevent too much line broadening by direct interaction, and to prevent absorption of all the pump light in a thin outer layer.

The best known and first laser (Ref. 5) is made of pink ruby, or Cr^{+++} ions in an Al_2O_3 host. While it has broad absorption bands (green and ultraviolet) like the ideal material of Fig. 1, its energy levels deviate from ideal in that the lower of the two maser levels is also the ground state. This means that population inversion cannot be obtained unless the ruby is pumped so hard that more than half the ions are driven into excited states. The emission is deep red, 6943 Å. Present pink ruby lasers have reached 50 joules of energy output per pulse. Pulse decay times range from 1 ms down to 0.12 μs by special "Q-switching" techniques. Peak power as high as 3 Mw has been reported. Fractional line width $\Delta f/f$ is typically 7×10^{-6}.

Laser action has been demonstrated in uranium (Refs. 6, 7, 8) (2.65 μ) and a number of rare earths, Sm (Refs. 9, 10), Nd (Refs. 11, 12, 13), Ho (Ref. 14), Tm (Refs. 15, 16), Dy (Ref. 17), Er (Ref. 18), and Pr (Ref. 19), all in the infrared. Host materials include $CaWO_4$, CaF_2, BaF_2, $SrMoO_4$, SrF_2, and glass. Resemblance between the energy levels and the ideal in Fig. 1 is usually rather remote. Extra levels are present, and the absorptions are not as broad as desired. One hopeful line of research is organic complexes containing rare earth ions. Chelates of rare earths have been shown to transfer energy from the broad absorption band in the organic to the discrete energy levels in the rare earth ion (Ref. 19).

Gases. The He-Ne gas laser is not pumped by another light source (Ref. 20). It consists of helium and neon gases

mixed at a pressure the order of 1 mm and contained in a tube the order of 1 m in length. Reflecting end plates may be internal or external to the tube. Metal sleeves on the outside of the tube couple in rf power that excites the gas and makes the tube glow like a neon lamp. A coincidence in energy levels of He and Ne allows excited He to transfer energy to Ne; this serves as the pumping mechanism. As Ne decays through its energy levels, an inverted population occurs at 11,500 Å, which breaks into oscillation. The oscillation is very narrow band, as narrow as 30 cps for a single mode, but the power level is low, on the order of 10 Mw of continuous wave.

C. Optical Circuit Elements

Now that the generation of coherent light has put optics in the realm of radio communications, it is natural to discuss a variety of optical circuit elements that are analogous to radio frequency circuit elements. The laser has already been discussed as a generator. If the reflecting end plates are omitted (no feedback) and incoming light is transmitted straight through the active material, then the laser becomes a traveling wave amplifier (Ref. 21).

Any light detector also serves as a detector in the electronic sense of the word. The photocell is a strictly square-law detector. By counting photons, it gives an output proportional to power, i.e., the square of the light amplitude. One suggested mixing and detecting scheme is shown in Fig. 4 (Ref. 22). Here a signal enters from the left and strikes a semitransparent mirror, where it is superimposed on light from a local oscillator. The frequencies of the superimposed beams differ, so that beats result. The beats are detected in opposite phase by two photocells. The photocells in turn drive a differential amplifier. In the absence of signal, the output of a properly balanced system vanishes, because each photocell sends the same signal strength to the differential amplifier which subtracts one from the other.

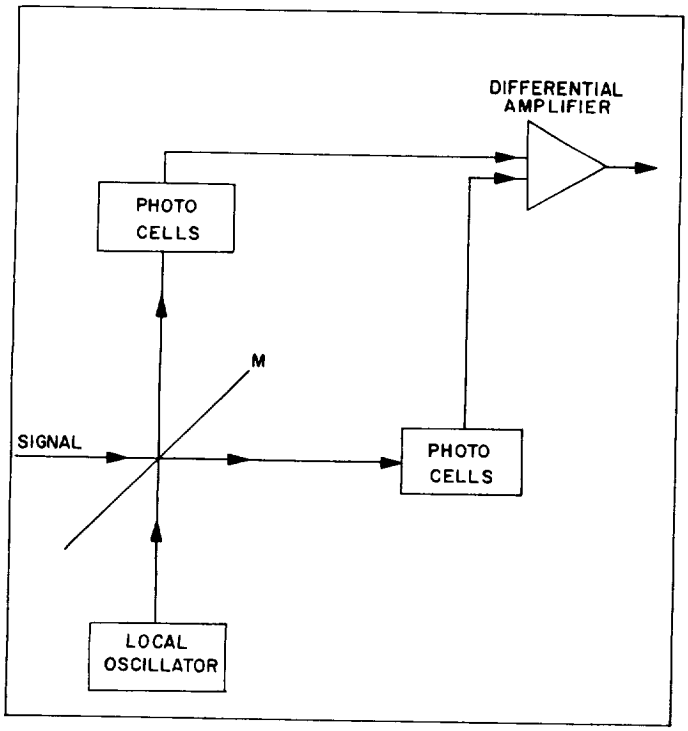

Fig. 4. Mixing and detecting scheme

Another means of photomixing was demonstrated by McMurthy and Siegman (Ref. 23). They operated a traveling wave tube on temperature-limited beam current, and focused the output of a ruby laser on its cathode. Several different modes of the laser were excited simultaneously. The beats of these modes were amplified by the traveling wave tube which gave outputs at 1800, 2400, 3600, and 4200 mc. The 600-mc frequency interval is in agreement with the calculated mode spacing, and the four frequencies listed above are all those multiples of 600 mc that fell within the bandwidth of the traveling wave tube.

Mixing has also been reported in crystals of substances that have nonlinear optical properties (Refs. 24 and 25).

A theoretical possibility for optical mixing that has not been verified experimentally (to our knowledge) is the mixing action of a three-level quantum system (Ref. 26). When an atomic system has three energy levels between which radiative transitions are allowed, and when it is irradiated (coherently) at two of the resonant frequencies, then it exhibits an oscillating polarization at the third resonance. The phase of the oscillation is determined by the phases of the exciting radiations. The oscillating polarization radiates a wavelet, which phases with other wavelets from other atoms to produce a net macroscopic output at the sum or difference frequency as shown in Fig. 5.

A variety of electro- and magneto-optic effects are available for modulating light. Kaminow (Ref. 27) has reported microwave modulation by means of the electro-optic effect in KH_2PO_4 (KDP). In his experiment, the KDP rod was in a microwave cavity with windows for the light, which propagated along the optic axis of the crystal. A polarizer and crossed analyzer prevented light transmission when the microwave field was off. When the field was on, two directions in the crystal (at 45 deg

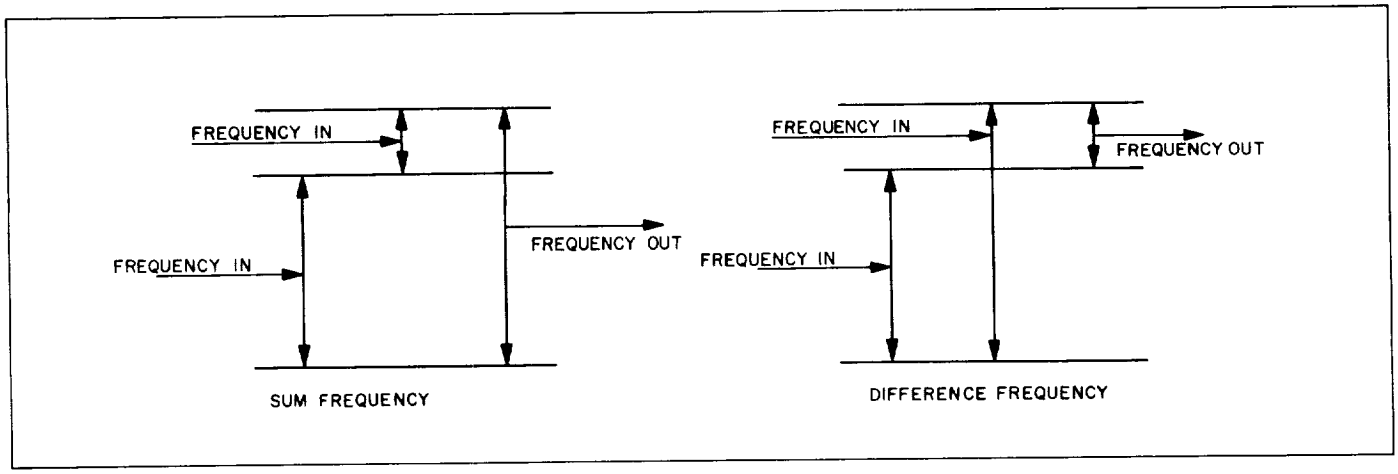

Fig. 5. Three-level mixer

to the polarizer and analyzer directions) had differing indices of refraction. The component of light polarization along these crystal directions shifted phase to make the light circularly polarized so that some was passed by the analyzer. For a sufficiently intense field, the KDP would become a half-wave plate and pass all the light. Of the two running wave components of the standing microwave, the one running parallel to the light was matched in phase velocity. The antiparallel component had little effect.

Another possible scheme for modulating a laser output is shown in Fig. 6. A square laser rod has totally reflecting end plates. The output is extracted from the side by having an oblique discontinuity in the refractive index that reflects a few percent (the rod could be cut and glued back together). A reflecting block shown at the top of the figure acts like the third arm of an interferometer. By making this block of appropriate material, its optical path length can be modulated by an electro-optic or piezoelectric effect. This modulates the interference of the two output paths.

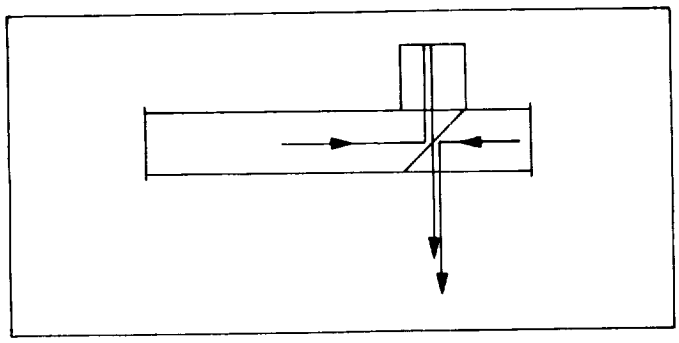

Fig. 6. Modulation scheme

The optical analog of a waveguide is the optical fiber. It is a thin fiber of glass (which may be clad with a glass of lower refractive index), that propagates light longitudinally by total internal reflections at the surface. Since laser action has already been demonstrated in a glass fiber (Ref. 13), it appears feasible to use optical fibers as wave guides that have gain. Optical "pipes" have also been investigated (Ref. 28). Of course, the simple obvious way to propagate light from one circuit element to one nearby is by free-space radiation, a method seldom used with nearby microwave circuits elements, since microwaves are not sufficiently directional.

In microwave technology, important uses have been found for ferrite devices in which waves are not reversible. Power entering one port of a circulator emerges from a second, but power entering the second does not emerge from the first, but rather from still another port. It is feasible to make the optical analog of this device by taking advantage of Faraday rotation. This effect is the rotation of the plane of polarization of light as it passes through a refractive medium in a direction parallel to a very intense magnetic field. Materials that exhibit a strong Faraday effect typically rotate the polarization 0.1 minute of arc per gauss per cm of path length. Qualitatively, one can understand the effect by thinking of the electric vector of the light vibrating the electron clouds in the atoms of the refractor.

The electrons do not vibrate straight, because the magnetic field exerts a force perpendicular to the velocity of vibration. The resultant of all the wavelets emitted by crooked vibrations of atoms, plus the original wave, is a light wave of rotated polarization.

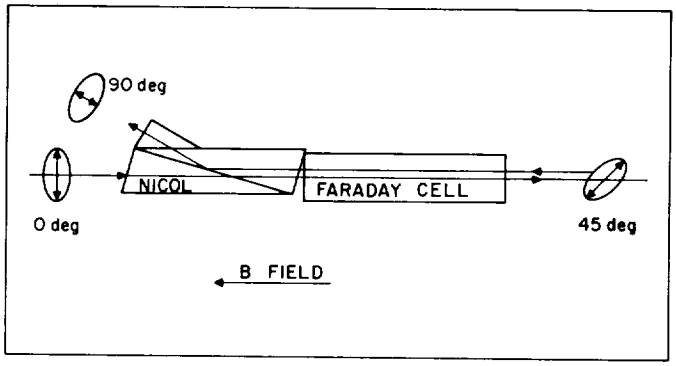

Fig. 7. Optical circulator

An optical "circulator" is depicted in Fig. 7. Vertically polarized light is shown passing through a Nicol prism, then through a Faraday cell. It emerges rotated by 45 deg, but light of the same 45 deg polarization returning through the cell will be rotated another 45 deg and will be "rejected" by the Nicol.

We have discussed the optical analogs to major circuit elements of microwave electronics. There are microwave components for which this analog is not feasible. In particular, spectrum coverage is lacking at present, since lasers are not tunable over an appreciable fraction of the spectrum. This creates difficulties in applications that involve large doppler shifts. The problem may in time be solved by optical parametric amplifiers (oscillators).

To complete the comparison, note that optical techniques are common for which the analogous microwave techniques would be very difficult, owing to the fact that microwaves emerging from laboratory-size apertures are not very directive. These techniques include repeated image formation, so common in optical instruments, rapidly rotating mirrors synchronized with pulsed signals, high resolution diffraction gratings, etc.

The applicability to space communications of systems made from optical components will be discussed next.

III. LIGHT AND RADIO SPACE COMMUNICATIONS

A. Spacecraft Communications

In this section, we consider communications with unmanned lunar and planetary spacecraft missions during the next seven years.

The spacecraft communication circuit includes spacecraft to Earth—the primary data transfer and tracking link, and Earth to spacecraft—the command link. Normally, this will be an integrated circuit providing coherent two-way transmission, to enable precision range and velocity measurements. Our experience with experimental spacecraft has convinced us that this link must provide two modes of operation simultaneously. The first mode (I) uses a directive spacecraft antenna to provide a high data rate when all is well with the spacecraft orientation system and the directive antenna can be properly pointed at the Earth. The second mode (II) uses an omnidirectional spacecraft antenna to provide a limited but useful data rate during the times that the spacecraft is not able to point a directive beam at the Earth (due either to maneuvers that the spacecraft is executing or a failure of part or all of the spacecraft orientation system).

Figure 8 shows the capability of data transfer from a spacecraft at the Moon or at Mars using a radio-frequency system. The figure is representative of past, present and predicted near future characteristics of the NASA/JPL Deep Space Instrumentation Facility (DSIF) and related spacecraft equipment. Initially, the ground stations use 26-m diameter antennas and conventional mixer-preamplifier receivers at 960 mc; 64-m diameter antennas and traveling-wave maser amplifiers at 2.3 kmc are substituted later. The related spacecraft start with omnidirectional antennas (prior to use of stabilized spacecraft) and ¼-watt transmitters at 960 mc; the final configuration for a stabilized spacecraft (Mode I) uses a 2.7-m diameter antenna and 100 w of power at 2.3 kmc. Improvements in information encoding have been incorporated along the way. The Mode I capability predicted by the latter half of this decade is broadcast quality TV from the Moon[3], and slow-speed video from the planets (also, not shown on Fig. 8, a few bits per second from the edge of the solar system).

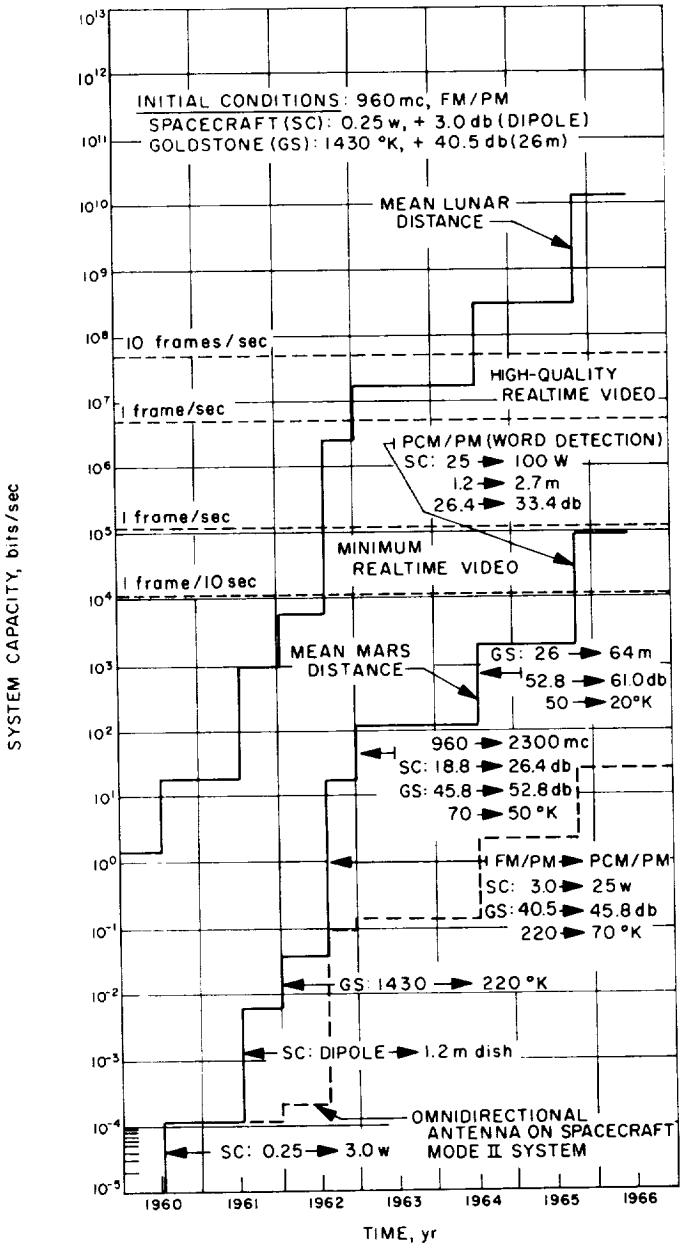

Fig. 8. Rf systems capability, space–Earth

Figure 8 also shows the case of omnidirectional transmission (Mode II) from Mars. The lesser capability of this mode shows when the spacecraft start to have practical stabilization capability (1961 on graph); also, no advantage is gained by the increase in operating frequency from 960 to 2300 mc (1963). There is no useful capability from the omni system much beyond the distance to Mars.

[3] One minor point to keep the record straight on Fig. 8 for the lunar communication case: if the Moon is in the beam, the system temperature would be increased about 25–30°K at 960 mc, 100–120°K at 2.3 kmc, and the system capability would be lowered accordingly.

The purpose of Fig. 8 is to illustrate that radio-frequency systems are developing satisfactorily to provide useful and apparently adequate spacecraft to Earth communications during the period of time considered.

The Earth to spacecraft link can be dispensed quickly. At any time in the evolution of the communication circuit, the threshold of the spacecraft receiver will be the order of 10 db poorer than the ground receiver; the ground transmitter power will be the order of 30 db better than the spacecraft. The net result is a nominal 20-db signal margin of the Earth to spacecraft over the spacecraft to Earth link. Also, the data requirements for the Earth to spacecraft link are lower, as they consist only of leisurely instructions to the spacecraft and the ranging modulation and doppler carrier.

There is no known requirement to send real-time pictures of the Earth out to a spacecraft near Mars. This is a fortunate situation, for the extra margin can be appropriately applied to simplification and increased reliability of the spacecraft receiver system.

The capability of the radio-frequency spacecraft communication system shows an increase of 10^9 times in the span of about six years. It is unlikely, however, that this rate of increase will be maintained for the subsequent six years into 1970, particularly since certain of the parameters (system noise temperature, ground antenna size) are apparently reaching somewhat hard natural physical or economic bounds. A further increase in size of the directive spacecraft antennas, however, is anticipated.

The limiting capabilities of an optical system are more obscure. Table 1[4] is a list of some of the parameters and predicted performance of an optical and radio (Earth-space-Earth) system for use in the 1965–1970 era. For Earth-space-Earth communications the atmosphere will cause the optical system to be only a fair-weather friend; however, this does not prevent our estimating its capability when it is usable.

The choice of parameters for Table 1 is justified as follows: A ground station transmitted power of 100 kw average is taken for both systems (Item 1). This is the anticipated power level of the DSIF rf system by the late sixties, obtained with a single high-power amplifier tube. The optical power is generated by a number ($\sim$10) of 10 kw average power lasers ($\approx$10 Mw peak); the individual lasers are mounted together and feed one or more apertures. The spacecraft radiated powers are equal (100 w average) for both systems. The validity of that

[4] See Appendix for constants and parameters used in calculating the table.

Table 1. Optical and radio spacecraft communication parameters (1965–1970)

	Item	Earth-Space Link		Space-Earth Link	
		2.1 kmc RF	Visual $\lambda = 0.694\mu$	2.3 kmc RF	Visual $\lambda = 0.694\mu$
Mode I System	1. Transmitter power (avg.)	100 kw (+50 dbw)	100 kw (+50 dbw)	100 w (+20 dbw)	100 w (+20 dbw)
	2. Transmitter antenna gain	60.2 db	103 db	33.4 db	103 db
	3. Power density at receiver	-130.4 dbw/m^2	-87.6 dbw/m^2	-187.2 dbw/m^2	-117.6 dbw/m^2
	4. Receiver antenna effective area	3.0 m^2	7.6×10^{-4} m^2	1.7×10^{3} m^2	13.1 m^2
	5. Received power	-125.6 dbw	-118.8 dbw	-154.9 dbw	-112.7 dbw
	6. Receiver noise spectral density	-204.0 dbw/cps	[a]	-214.5 dbw/cps	[a]
	7. Bandwidth for $S/N = 6$ db at 300×10^6 km	1.7×10^7 cps	$1.5 \times 10^4 - 1.115 \times 10^6$ cps	2.3×10^5 cps	$5.9 \times 10^4 - 4.8 \times 10^6$ cps
Mode II System	8. Transmitter antenna gain	60.2 db	103 db	0 db	0 db
	9. Power density at receiver	-130.4 dbw/m^2	-87.6 dbw/m^2	-220.6 dbw/m^2	-220.6 dbw/m^2
	10. Receiver antenna effective area	-1.6×10^{-3} m^2	7.6×10^{-4} m^2 [a]	1.7×10^3 m^2	13.1 m^2
	11. Received power	-158.4 dbw	-118.8 dbw from signal -121.6 dbw from Sun	-188.3 dbw	-215.7 dbw
	12. Bandwidth for $S/N = 6$ db at 300×10^6 km	9.1×10^3 cps	S/N $\approx$3 db with gating[a]	1.05×10^2	$S/N << 1$ ($\approx 10^{-3}$ photons/sec)

[a] See text.

prediction depends upon the relative power to weight ratio for the different systems. We have not made design tradeoff studies on any such problems as yet.

The rf system uses a 64-m diameter ground station antenna (Item 2) which will have similar electrical performance capabilities to the CSIRO 64-m (210 ft) radio-astronomy antenna now in operation at Parkes, Australia. The optical system will use 4-cm diameter apertures in the ground transmitter. The apertures will provide a maximum gain of 103 db corresponding to a beamwidth of 5 seconds of arc. This is expected to be the greatest gain usable due to the angular scintillation of the signal by the atmosphere (which is order 5 sec* much of the time—remembering the system must look to large zenith distances). Pointing the 5 sec* beam requires an accuracy of 0.5 to 1 second of arc to stay well up on its "flat" top; no doubt, active optical angle tracking of the spacecraft signal will be required to provide suitable steering instructions for the transmitting telescope.

The rf spacecraft antenna (Item 2) for Mode I is a 2.7-m diameter aperture with a half-power beamwidth of about 4 deg; it requires a pointing accuracy of about 0.4 to 0.8 deg for proper operation. This accuracy is provided by the nominal orientation accuracy of the spacecraft. The minimum beamwidth of the spacecraft optical system is not determined by optical seeing, it is determined by the limiting accuracy of tracking by the optical receiving system and the collimation accuracy between the received and transmitted beams—the optical receiver angle tracks the received signal and uses the information to steer the transmitted optical beam. From this reasoning we arrive at a minimum optical system beamwidth of about 5 sec* of arc (25×10^{-6} rad). That beamwidth corresponds to an optical system transmitting antenna gain of 103 db obtained with a ~4 cm diameter aperture.

Item 3 of Table 1 shows the power density in the signal at the receiver in the various cases. The effective areas of the receiver apertures in Item 4 are then used to compute the received signal power (Item 5).

To compute the signal-to-noise ratio at the receiver the noise power must be known. A system noise temperature of $T = 25°K$ which includes all external and internal noise is used for the rf system ground receiver, $T = 290°K$ is used for the spacecraft receiver. These values are expressed as a noise spectral density in db relative to one w/cps (Item 6).

The optical system noise comes from randomness in the arrival time of the visual photons and from background noise picked up in the telescope. We have assumed that equipment noise, i.e., photomultiplier dark current, etc, is negligible in the optical system. In the case of "infrequent" photons arriving at random times, the statistical fluctuation of the total number counted is $\Delta\bar{n}^2 = (n_s + n_b)\, t\varepsilon$, where n_s and n_b are the photons per sec in time t from the source and background, respectively, and ε is the quantum efficiency of the detector (ratio of output events to input photons). The mean squared signal-to-noise power is:

$$\left(\frac{S}{N}\right)^2 = \frac{n_s^2\,(h\nu)^2\, t^2\varepsilon^2}{(n_s + n_b)\,(h\nu)^2\, t\varepsilon} = \frac{n_s^2 t\varepsilon}{(n_s + n_b)} \qquad (1)$$

the ratio of squared signal power to mean square fluctuations of total power received (Ref. 29). As an example of the use of formula (1) we have calculated the approximate threshold sensitivity of a 5.1 m (200 in.) telescope using photographic film for detection. The results and the various assumptions used are shown in Fig. 9.

In order to connect Eq. (1) to the bandwidth concept, the counting time t should be taken as one $(2B)^{-1}$, a half period of the information bandwidth.

Noise analyses have been carried out for two other light receiving schemes besides the direct photon counting represented by Eq. (1). One is the coherent mixing of the incoming signal with light from a local oscillator. This is done in partial mirrors, and the resulting beats are detected photoelectrically. The other scheme is a coherent linear amplification by means of a laser amplifier prior to detection. The mixer-detector has been studied by Oliver (Ref. 22 and 30). Haus, Townes, and Oliver have made an interesting comparison of the latter two schemes and have demonstrated that the idealized devices have the same S/N ratios for a given information bandwidth (Ref. 30 and 31). In any case, marginal reception corresponds to the idea that at least one $h\nu$ of power must be received in each time interval $(2B)^{-1}$ or in other words, signal power must exceed the noise power of $h\nu B$, equivalent to a noise temperature of $h\nu/k$ (Ref. 32, 33).

An upper limit on the S/N obtainable with a coherent amplifier is thus

$$\frac{S}{N} = \frac{\text{signal power}}{\text{noise power}} = \frac{P_s}{h\nu B} \qquad (2)$$

The bandwidth entries in Table 1 were calculated for the visual system using both Eq. (1) and (2).

It should be noted that practical factors degrade the performance of the photoelectric detector systems in a way that differs from the degradation of the linear maser

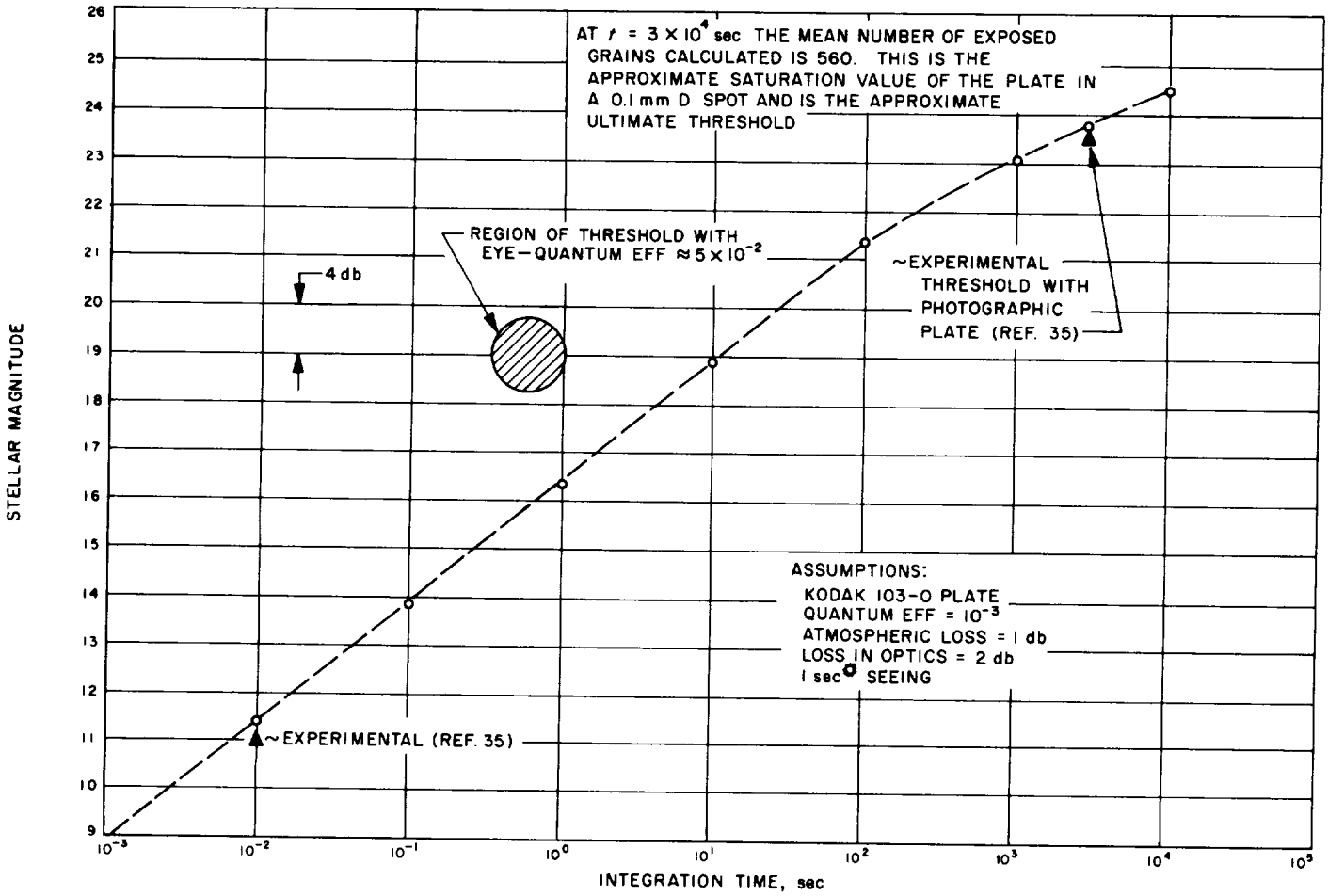

Fig. 9. Threshold magnitude of telescope

amplifier. The ratio S/N is decreased by the factor ϵ, the quantum efficiency, in the photoelectric cases, simply because there is a probability $(1 - \epsilon)$ of failure to detect each quantum. In the maser case, however, the noise is traced to spontaneous emission from the active atomic systems. One may discriminate against this noise insofar as its angular direction differs from that of the signal, but if the signal is spread in angle by imperfect optics, or atmospheric disturbance, then the ability to discriminate is accordingly reduced. More precisely, one should speak of the manner in which the signal is distributed among the traveling wave modes of the optical system and the number of such modes that are admitted to the final detector. Each mode carries a noise power of $h\nu$ per unit bandwidth.

The mechanization of the visual system is assumed to be pulse position or amplitude modulation of ~0.5 ms pulses from the laser with average power as in Item 1 of Table 1. The pulses of photons entering the receiver are multiplied by a local model of the pulse wave form to provide background discrimination and detection of the initial modulation. Actually, Mode I systems will not normally suffer from any background noise problems, so, from the point of view of discrimination against background noise, the "coding" of the transmitted wave form is unnecessary.

The bandwidths B, for the rf links were based on coherent detection of the signal in random noise calculated in a conventional manner,

$$\frac{S}{N} = \frac{\text{signal power in } B}{\phi B}$$

The capabilities of the Mode I systems can be compared on the basis of the entries of Item 7. For the rf system Table 1 can be found in agreement with the 1966 information in Fig. 8.

For the Mode II case (omnidirectional spacecraft transmitter and receiver antennas) the entries to Table 1 for the rf system are calculated in the same way as for the Mode I entries. From the table we note that the Earth-space rf link enjoys about 20 db greater capability than the space-Earth-link, and the space-Earth link has limited capability—satisfactory for transferring the results of engineering measurements in the spacecraft (temperature, control system performance, etc) and/or slowly varying measurements of scientific phenomena.

For the optical Mode II system the case is considered of a passive omnidirectional receiving antenna in which the effective aperture is given by the fundamental relationship,

$$A = \frac{\lambda^2 G}{4\pi} = \frac{\lambda^2}{4\pi}$$

for $G = 1$. At $\lambda = 0.69\ \mu$, the area is quite tiny, $\sim 4 \times 10^{-14}$ m^2. Using the Mode II visual system parameters as listed, it takes about 10^4 seconds to establish a good probability of one signal photon being received. Because that omni system does not work, a passive system is considered which has multiple larger apertures to provide the omnidirectional coverage required.

At optical frequencies it is practical to use large aperture wide field of view devices (Kellner-Schmidt optics, for instance)—the photons collected by the aperture over its entire field of view are collected on an extended focal surface and their total can be counted. In this concept the spacecraft would have a number, e.g., 4 such apertures, each covering a different π steradians, and the photons from the four instruments would be added. Using 4-cm diameter apertures, about 4.6×10^6 signal photons would be collected per second. The Sun interferes with this system, however. It contributes about 10^{10} photons/sec to the 10^6 cps wide spacecraft optical receiver at Mars. The average signal power received (-118.8 dbw) is thus about 28 db below the average noise power received (-91.2 dbw). As noted previously, a coherent demodulation technique could and probably would be used. We may look at this process as a pre-detection range gate (blanking the receiver so the noise photons are not counted during the time signal pulses are not received); a discrimination of noise in preference to signal of ~ 30 db would result for a 10^{-3} duty cycle. Still, a total signal to noise power ratio of approximately unity would remain ($\approx +3$ db). In this case, with a very large number of signal and noise photons being collected, the criterion of detection is not related to the random photon count noise, but rather total signal and noise powers as in a low-frequency case of detection of noise in noise, i.e., as a radiometer for radio astronomy. Qualitatively, it would require several seconds to examine each of the 10^3 intervals in the range gate. Thus, we reach the not surprising conclusion that Mode II operation of the spacecraft visual receiver is not practical due to solar interference (Item 12). The space-to-Earth visual link with an isotropic optical source on the spacecraft does not provide sufficient signal at the ground receiver to be of any use (Item 12).

We may be concerned in the future with communication between two unmanned spacecraft, as for example the parent-offspring of a Mars orbiter-lander. The comparable data to Fig. 1 for this case has not been developed. However, the system would probably be designed at a relatively low frequency, perhaps 100 Mc, much like early Earth satellites, to allow effective operation with omnidirectional radiators on both spacecraft. It seems highly unlikely that spacecraft designers will favor use of an even rudimentary angle acquisition and stabilization system, at least in the early days of this family of spacecraft machines.

B. Lidar/Radar

We turn now to lidar/radar and consider Earth-based systems related to space exploration. Table 2[5] shows the parameters of the 2.4 kmc system used during the 1961 planetary radar experiment performed by JPL at the Goldstone Tracking Station (Ref. 34); the parameters of a future 2.3 kmc system (1965–1970), and the parameters of a possible contemporary[6] and a possible future (1965–1970) lidar system.

The parameters of the future rf system are similar to the ground station characteristics of the 2.3 kmc system just discussed for spacecraft communications (Table 1). A higher power is used for the radar (300 kw) than is considered needed for the communication transmitter (100 kw). The early optical system uses a pulsed laser (Item 1) with an average power of 10 w (one 100 joule pulse 10^{-3} sec long every 10 sec); it feeds a 0.2-m telescope giving an approximate 1 sec of arc beam (Item 3). Seeing

[5] See Appendix for constants and parameters used in calculating the table.

[6] During the preparation of this report a lidar contact with the Moon was reported by a group from the MIT and Raytheon Company under the direction of Prof. L. Smullin and Dr. G. Fiocco. Reported system parameters: four 0.69 Å lasers to give a 50 joule pulse in 5×10^{-4} sec, once per minute, 13 pulses radiated through 10 in. scope to dark part of Moon in early evening, 48 in. reflector and photomultiplier tube receiver.

Table 2. Parameters of 2388-mc radar and 0.69 μ lidar systems

Item	RF System 1 (Venus 1961)	RF System 2 (1965–1970)	Optical System 1 (Circa 1962)	Optical System 2 (1965–1970)
1. Transmitter average power output	+41.1 dbw 13 kw	+54.8 dbw 300 kw	+10 dbw 10 w	+50 dbw 10 Individual at 10 kw
2. Transmitter telescope configuration	26-m reflector	64-m reflector	0.2-m reflector	10 Individual 0.2-m reflectors
3. Telescope beamwidth	~0.33 deg	~0.14 deg	~1.0 sec* solid $\measuredangle = 2.5 \times 10^{-11}$ stere	~1.0 sec* solid $\measuredangle = 2.5 \times 10^{-11}$ stere
4. Minimum width of transmitted spectrum	<1 cps	<1 cps	~6×10^5 cps	~10^6 cps
5. Receiver telescope configuration	26-m reflector	64-m reflector	5.1-m reflector	5.1-m reflector
6. Receiver system capability	49°K receiver system noise temperature	10°K receiver system noise temperature	Quantum eff = 10^{-2}	Quantum eff = 10^{-1}
7. Receiver minimum pre-detection bandwidth	5 cps	5 cps	~6×10^8 cps	~10^6 cps

conditions must be good (~1 sec) for the tabulated performance to be valid (1 sec seeing conditions are typically one night in four for the Mt. Palomar Observatory in California [Ref. 36]). The bandwidth of the laser pulse quoted is typical of current devices (Item 4). The telescope used for the receiver has a diameter of 5.1 m (200 in.) as represented by the large reflector at the Palomar Observatory (Item 5). A value of 10^{-2} is used for the detector quantum efficiency (Item 6). That performance is in the middle range between current photographic plates and photomultipliers (Refs. 29, 36).

The input bandwidth of the receiver is set by a passive filter; the function of the filter is to eliminate extraneous light but still efficiently pass the comparatively narrow band laser pulse; the resolution of 6×10^8 cps is currently achievable.

The optical system (2) for 1965–1970 has an average power of 100 kw obtained either by operating 10 or 100 lasers at 10 or 1 kw, respectively, feeding one or more 0.2-m diameter reflectors. We assume an improvement to 10^{-1} for the quantum efficiency of the detector, and a receiver input filter with good transmission and of sufficient selectivity to match the purity of the transmitted laser pulse ($\Delta\nu = 10^6$ cps). Perhaps a laser amplifier could do that job.

Table 3[7] shows the predicted performance of the two radar systems on the Moon, Venus, and Mars. Not much data were taken on the Moon with the 1961 system, since most of the time available during the experiment was

[7] See Appendix for constants and parameters used in calculating the table.

Table 3. Predicted performance of 2388-mc lunar/planetary radar systems

Item	RF System 1 (JPL 1961)			RF System 2 (1965–1970)		
	Moon	Venus[a]	Mars	Moon	Venus	Mars
1. Power intercepted by target (average)	+38.6 dbw	+11.9 dbw	+1.1 dbw	+51.8 dbw	+33.6 dbw	+22.8 dbw
2. Power delivered to receiver	−135.6 dbw	−196.4 dbw	−211.7 dbw	−114.5 dbw	−166.8 dbw	−182.1 dbw
3. Background noise	115°K	15°K	15°K	125°K	11°K	10°K
4. Total noise	164°K (= −206.5 dbw/cps)	64°K (= −210.6 dbw/cps)	64°K (= −210.6 dbw/cps)	135°K (= −207.3 dbw/cps)	21°K (= −215.4 dbw/cps)	20°K (= −215.6 dbw/cps)
5. Signal bandwidth	~10^2 cps	~10 cps	~10^3 cps (?)	~10^2 cps	~10 cps	~10^3 cps (?)
6. Time for S/N = 6 db[c] or S/N in signal bandwidth	S/N = +50.9 db	t = 4.7 s[b] S/N = +4.2 db	$t = 5.4 \times 10^4$ s[b] S/N << 0 db	S/N = +72.8 db	S/N = +38.6 db	$t = 6.5 \times 10^{-3}$ s S/N = +3.5 db

[a] Actual performance of 1961 system on Venus.
[b] Used 50% duty factor off-on keying; 25 cps pre-detection bandwidth used on Venus, 10^3 cps assumed for Mars.
[c] At conjunction.

used for making measurements on the planet Venus (Ref. 34). The Moon was used to test the system and the predicted threshold was experimentally verified. Also, in the few data runs made on the Moon with the 1961 system, good returned signal spectra essentially out to the limbs of the Moon (1 cps resolution in the central spike) were obtained, and measurements of the magnitude and spectrum of the depolarized component of the reflected signal were made.

The results obtained from Venus with the 1961 system are of considerable scientific importance: an accurate value of the astronomical unit was obtained (149, 598, 500 ± 500 km) by precision range and coherent doppler velocity measurements; depolarization measurements provided an estimate of the surface roughness at the scale of a wavelength at 2.4 kmc (roughness similar to the Moon); accurate returned signal level measurements provided a determination of the ratio of the radar to geometrical cross section of Venus (-9.5 ± 1 db for zero propagation loss, ambiguous to the extent the propagation losses are not known); returned signal spectral measurements to a resolution of 1 cps, which, combined with the depolarization measurements, provided an estimate of the Venus rotation period (returned spectrum half power width ~6 cps, 225 day rotation period estimated).

No attempt was made to observe Mars with the 1961 system as Mars was far from conjunction at the time of the experiment. It would probably have been futile (Item 6).

The 1965–1970 rf system (2) in Table 3 predicts: a capability for highly refined measurements on the Moon; sufficient signal from Venus to track it through its year (Venus varies by ~32 db on an Earth-based radar power meter from superior to inferior conjunction); Mars will come solidly into view. The ability to track Venus continually through its orbit may be very significant; it would probably lead to firm resolution of the axis orientation of Venus and her rotation period, it would surely lead to a better calibration of the solar system (AU, etc). Very good signal spectrum, signal depolarization and power vs. range in the echo should be available at Venus inferior conjunction. The fruits of measurements on Mars may be less significant because more information on that planet is already available from reflected Sun optical measurements; it is evident that precision range measurements, signal depolarization measurements, and accurate reflected signal strength and signal spectrum measurements should be available.

Table 4 is a résumé of the performance potential of the lidar systems. The system available this year is limited to marginal detection of the Moon and perhaps an indication of things to come. The lidar system for which the technology could be available in 1965–1970 can contact Mars, measure Venus, and perhaps explore the Moon to a degree not then accomplished by other means. It is not known if any specific new scientific knowledge applicable to planetary spacecraft exploration could be derived with the lidar on Venus and Mars at the performance levels

Table 4. Performance of 0.69 μ lunar/planetary lidar systems

Item	Optical System 1 (1962)			Optical System 2 (1965–1970)		
	Moon	Venus	Mars	Moon	Venus	Mars
1. Power intercepted by target (average)	$+192.4$ dbPs^{-1} [a] ($= +7$ dbw)	[c]	[c]	$+232.4$ dbPs^{-1} ($= +47.0$ dbw)	$+232.4$ dbPs^{-1} ($= +47.0$ dbw)	$+232.4$ dbPs^{-1} ($= +47.0$ dbw)
2. Power delivered to receiver	$+8.4$ dbPs^{-1} ($= -177.0$ dbw)	[c]	[c]	$+49.4$ dbPs^{-1} ($= -135.9$ dbw)	$+19.8$ dbPs^{-1} ($= -165.6$ dbw)	$+5.3$ dbPs^{-1} ($= -180.1$ dbw)
3. Noise at receiver[b] from background	$+8.4$ dbPs^{-1} ($= -177.0$ dbw) ~20 db less for dark Moon	[c]	[c]	-19.4 dbPs^{-1} ($= -204.8$ dbw)	-17.6 dbPs^{-1} ($= -203.0$ dbw)	-19.9 dbPs^{-1} ($= -205.3$ dbw)
4. Total noise (not including quantum noise)	← Equipment noise (film fog, photomultiplier dark current, etc.) assumed negligible →					
5. Input bandwidth	6×10^8 cps	[c]	[c]	10^6 cps	10^6 cps	10^6 cps
6. Time for S/N = 6 db at output	2.3×10^2 sec (dark Moon) 4.5×10^2 sec (lighted Moon)	[c]	[c]	1.8×10^{-3} sec[d] $B = 2.24 \times 10^4$ [e]	1.7 sec	47 sec

[a] The unit dpPs^{-1} is decibels relative to one photon per sec.
[b] Noise quoted 30 db below actual incident noise level, accomplished by receiver gating of laser pulses.
[c] Not practical.
[d] From Eq. 1.
[e] From Eq. 2.

shown for system 2. The lunar performance looks more intriguing. Item 2 shows $+49.5$ dbPs$^{-1} = 8.7 \times 10^4$ photons/sec sent to the receiver; at that rate, in 1.8×10^{-3} sec an S/N of 4 is produced, i.e.,

$$\frac{S}{N} = \sqrt{n_s t_f} = \sqrt{8.7 \times 10^4 \times 1.8 \times 10^{-3} \times 10^{-1}} = \sqrt{16} = 4$$

(for the negligible background case, incoherent detection)

Suppose a pulsed laser transmitter is used providing one 1 ms pulse of 8.7×10^4 photons at the receiver each second. Then, in a 1.8 μsec interval of the pulse we produce an S/N of 4, i.e.,

$$\sqrt{1.8 \times 10^{-6} \times 8.7 \times 10^4 \times 10^3 \times 10^{-1}} = \sqrt{16} = 4$$

Thus, if the original 1 ms pulse is chopped at a (1.8 μsec)$^{-1}$ rate we could in principle perform range measurements of a 1.8 μsec resolution (270 m) with an S/N of 4 in each 1.8 μsec portion of transmitted pulse. Assuming a 50% duty factor of the chopping, $\sim$280 such samples would be collected in each second to improve the signal-to-noise ratio to $\sim 4\sqrt{280}$ in a second. There are certainly large technological problems to doing what has just been described (and if it were done, it would probably be done in a different manner than that described) but the point we wish to make is that in concept precision range measurements to the Moon surface could be made with the system 2 lidar. Lidar is potentially superior to radar for ranging the Moon, because the radar range is averaged over a large area, whereas the lidar beam only intercepts about 4 km^2.

However, shadow analysis has already surpassed the predicted 1965–1970 lidar potential for vertical resolution of the *detailed* shape of the Moon. The trained eye under ideal seeing conditions can resolve about 1 km normal to the line of sight (horizontal distance at the center of the lunar disc). By taking advantage of very long shadows, which occur at various phases of the Moon, the vertical resolution can be improved to about 10 m, a factor of 100. Of course, the cumulative effects of gradual slopes do not show in shadow analysis. For this reason lidar could be uniquely useful in studying certain features of the Moon's surface. If we assume as a first approximation that the Moon is a spheroid, then lidar could provide the means for measuring the diameter along the line of sight. Other data of probably less importance could result from lunar lidar, e.g., depolarization of light upon reflection is a clue to surface character, and vertical resolution of objects that are shaded by larger objects is possible.

IV. CONCLUSIONS

This report has: surveyed laser oscillators and some selected optical devices; considered the evolution of a radio-frequency space communication system (Earth-space-Earth) in the 1960–1970 period; compared the predicted characteristics of rf and optical Earth-space-Earth communications systems for 1965–1970; commented on a particular space-space communication problem; compared the (mostly) predicted characteristics of lunar/planetary radar and lidar for 1961–1970 and made some remarks on their absolute (rather than relative) usefulness. Space-borne altimeters or other spacecraft navigating or landing aids were not considered.

The following conclusions relevant to the 1965–1970 period are drawn:

1. Lasers open a new regime of spectral purity in the optical frequencies and a new regime in energy density. They must surely have a good future in scientific research.

2. Radio-frequency systems are better than optical systems for Earth-spacecraft-Earth communications. Radio systems provide reasonable capability for solar system spacecraft.

3. Future lidars could provide unique information about the Moon's surface and its selenoid. Lidars are not likely to provide much in planetary exploration, whereas radars will.

APPENDIX

I. CONSTANTS AND EQUATIONS FOR TABLE 1

The following are used for calculating Items 2–5 and 9–11 of Table 1:

$$P_R = \frac{P_T G_T A_R}{4\pi R^2} \times L \qquad \text{(A-1)}$$

R = range (meters)

P_R = power received (watts)

P_T = power transmitted (watts)

G_T = transmitter antenna gain

A_R = effective area of receiver antenna (m^2)

$$A_R = \eta A = \eta \frac{\pi (\text{diameter of aperture})^2}{4} \ (m^2)$$

η = aperture efficiency

η_{rf} = −2.8 db (includes all feed line losses)

η_{opt} = −2 db (includes optical losses)

L = atmospheric losses

$L_{rf} \cong 0$ db

L_{opt} = −1 db (one way through atmosphere)

The Sun's interference into the omni antenna system was calculated from data on pp. 138, 140 of Ref. 36:

solar noise = 1.0×10^{-12} dbw/m^2/cps at Mars

The following are used for calculating Items 7 and 12 of Table 1:

$$\left(\frac{S}{N}\right)_{rf} = \frac{P_R}{\Phi_N B} \qquad \text{(A-2)}$$

Φ_N = noise spectral density for rf system (w/cps)

$\Phi_N = kT = -204$ dbw/cps, for $T = 290°K$

$k = 1.380 \times 10^{-23}$ joules/°K (Ref. 36)

B = bandwidth (cps)

$$\left(\frac{S}{N}\right)^2_{optics} = \frac{n_s^2 t\epsilon}{(n_s + n_b)} \qquad \text{(Eq. 1 of text)} \qquad \text{(A-3)}$$

n_s = mean number of signal photons/sec presented at input to optical receiver

$n_s = \frac{P_R}{h\nu}$

ν = frequency (cps)

$h = 1.380 \times 10^{-23}$ joules/°K Planck's constant (Ref. 28)

$n_s = SA_R \eta_{opt}$

S = photons/m^2/sec incident on telescope (signal)

n_b = mean number of background photons/sec presented at input to optical receiver

$n_b = A_R b \eta_{opt}$

b = background photons/m^2/sec incident on telescope

Also,

$$\frac{S}{N} = \frac{P_R}{h\nu B} \qquad \text{(Eq. 2 of text)} \qquad \text{(A-4)}$$

II. CONSTANTS AND EQUATIONS FOR TABLE 2

The following applies to Item 3 of Table 2:

$$\text{beamwidth} \cong \frac{\text{wavelength}}{\text{diameter of effective aperture}} = \frac{\lambda}{D_e} \text{ radians}$$

III. CONSTANTS AND EQUATIONS FOR TABLE 3

The following applies to Item 1 of Table 3:

$$P_{int} \cong \overline{P_T} \times \Omega \qquad \text{(A-5)}$$

P_{int} = power intercepted by target (watts)

P_T = average power transmitted/stere in Ω

= 2.8 db below peak power/stere for rf systems on Moon

Ω = solid angle of target (steradians)

The following applies to Item 2 of Table 3:

$$P_R = \Gamma \frac{P_{int}}{4\pi R^2} A_R L_{rf} \text{ watts} \qquad \text{(A-6)}$$

$$\Gamma = \frac{\text{target radar cross section}}{\text{target geometrical cross section}}$$

= −16 db for Moon (Ref. 26)

= −9.5 db for Venus (Ref. 26)

= −8.2 db for Mars (Albedo, Ref. 28)

Background noise (Item 3) is from thermal radiation of target and atmosphere in receiver beam, and Earth radiation into receiver side lobes.

Total noise (Item 4) is sum of background and receiver noise (from Item 6 of Table 2).

Signal (3 db) width (Item 5) for Moon and Venus from Ref. 26. For Mars it is calculated from the Venus signal width times the ratio of Mars to Venus rotation rate times the ratio of Mars to Venus diameter.

S/N in signal (~3 db) bandwidth (Item 6) calculated from Eq. (A-2). Time for S/N to reach 6 db on planets is calculated from equation on page 41 of Ref. 34.

IV. CONSTANTS AND EQUATIONS FOR TABLE 4

Item 1 calculated using A-5 with $P_T = P_T \eta_{opt} L$, and $\Omega = 25 \times 10^{-11}$ steradian.

Item 2 is calculated using Eq. (A-6) with Γ = albedo of planet; $\Gamma = 0.07$ for Moon, 0.61 for Venus, 0.150 for Mars (Ref. 36), and $L_{opt} = -1$ db.

The approximate background noise from the dark Moon was calculated from solar light scattered by ¼ of the Earth and reflected by the Moon. The background from Mars was calculated from solar illumination in the 1-sec spot size (Mars at opposition). Solar constants, albedos from Ref. 28.

The background viewing Venus is calculated from the Sun's aureole at 10 deg from the center of the Sun (p. 68 of Ref. 29), i.e., Venus near inferior conjunction.

The entries to Item 6 are calculated from Eq. (A-3) and (A-4).

V. CALCULATIONS FOR FIG. 9

The flux corresponding to a zero photographic magnitude star, s_0, $\cong 10^{10}$ photons/m²/sec outside the Earth's atmosphere was calculated from the flux, $f\lambda$, and spectral width $P\lambda$.

$\log f\lambda\,(pg) = -0.4m_{pg} - 8.3$ erg/cm²/Å/sec, near $\lambda = 4{,}300$ Å (p. 174 of Ref. 33)

$P\lambda\,(pg) \cong 1290$ Å (p. 178 of Ref. 33)

$f\lambda\, P\lambda =$ total flux (erg/cm²/sec)

The signal power to the telescope detector (Kodak 103-0 plate) is:

$$n_s = A\,\eta_{opt}\,L_{opt}\,s$$

$s =$ incident flux from star above atmosphere in photons/m²/sec ($s_0 = 10^{10}$ photons/m²/sec)

$A \cong$ area of 200-in. telescope $= 20.4$ m²

The noise from the background sky, n_b', photons/sec is

$$n_b' = Ab\,\Omega\,\eta_{opt}\,L_{opt}$$

$b =$ is background flux from dark sky in photons/sec/m²/steradian

$= 5.8 \times 10^{11}$ photons/m²/sec/stere (-4.4 mag/stere/m²)

$\Omega = 25 \times 10^{-11}$ stere (1-sec arc seeing conditions)

There is background noise n_b'' from film fog equivalent to $\approx 10^{-3}$ erg/cm² (2.2×10^8 photons/cm²) incident on the plate (estimated from Ref. 38). This background in the $\sim 10^{-4}$ cm² image size on the plate (corresponding to 1 sec of arc seeing) is 2.2×10^4 photons/image spot. Equation (A-3) can be solved for n_s,

$$n_s = \frac{(S/N)^2}{2\varepsilon t}\left(1 + \sqrt{1 + \frac{4\varepsilon t n_b}{(S/N)^2}}\right)$$

$$n_b = (n_b' + n_b''/t)$$

If $(S/N) = 4$ is taken as defining threshold, then,

$$n_s = \frac{8}{\varepsilon t}\left(1 + \sqrt{1 + \frac{t\,(n_b' + n_b''/t)}{4}}\right) \quad \text{at threshold} \tag{A-7}$$

Equation (A-7) was used to calculate the limiting magnitudes in Fig. 9. Since plate capacity is $\approx 5 \times 10^6$ grains/cm², a spot of 10^{-4} cm² is filled with about 500 events. This determines the ultimate threshold of the telescope with a plate of the assumed characteristics.

ACKNOWLEDGEMENT

The authors wish to thank W. K. Victor for informative discussions on lunar lidar.

REFERENCES

1. Fox, A. G., and T. Li, "Resonant Modes in a Maser Interferometer," *Bell System Technical Journal*, Vol. 40, No. 2, March 1961.
2. Boyd, G. D., and J. P. Gordon, "Confocal Multimode Resonator for Millimeter Through Optical Wave Length Masers," *Bell System Technical Journal*, Vol. 40, pp. 489–508, March 1961.
3. Kaiser, W., and C. G. B. Garrett, *Physical Review Letters*, Vol. 7, p. 229, 1961.
4. Franken, P. A., A. E. Hill, C. W. Peters, and G. Weinreich, *Physical Review Letters*, Vol. 7, p. 118, 1961.
5. Maiman, T. H., *Nature*, Vol. 187, p. 493, August 1960.
6. Sorokin, P. P., and M. J. Stevenson, *Physical Review Letters*, Vol. 5, p. 557, 1960.
7. Porto, S. P. S., and A. Yariv, *Journal of Applied Physics*, Vol. 33, p. 1620, 1962.
8. Boyd, G. D., et al., *Physical Review Letters*, Vol. 8, p. 269, 1962.
9. Sorokin, P. P., and M. J. Stevenson, *IBM 9 Research and Development*, Vol. 5, p. 56, January 1961.
10. Kaiser, W., et al., *Physical Review*, Vol. 123, p. 766, 1961.
11. Johnson, L. F., and K. Nassau, *Proceedings of the IRE*, Vol. 49, p. 1704, 1961.
12. Johnson, L. F., et al., *Proceedings of the IRE*, Vol. 50, p. 213, 1962, Correspondence.
13. Snitzer, E., *Physical Review Letters*, Vol. 7, p. 444, 1961.
14. Johnson, L. F., G. D. Boyd, and K. Nassau, *Proceedings of the IRE*, Vol. 50, p. 87, January 1962, Correspondence.
15. Johnson, L. F., G. D. Boyd, and K. Nassau, *Proceedings of the IRE*, Vol. 50, p. 86, January 1962, Correspondence.
16. Kiss, Z. J., and R. C. Duncan, *Proceedings of the IRE*, Vol. 50, p. 1532, June 1962.
17. Kiss, Z. J., and R. C. Duncan, *Proceedings of the IRE*, Vol. 50, p. 1531, June 1962.
18. Yariv, A., et al., Correspondence (to be published).
19. Crosby, G. A., R. E. Whan, and R. M. Alire, *Journal of Chemical Physics*, Vol. 34, p. 743, 1961.
20. Javan, A., W. R. Bennett, and D. R. Herriott, *Physical Review Letters*, Vol. 6, p. 106, February 1961.
21. Kisliuk, P. P., and W. S. Boyle, *Proceedings of the IRE*, Vol. 49, p. 1635, 1961.
22. Figure on cover of *Proceedings of the IRE*, Vol. 50, No. 2, Cover Story: B. M. Oliver, Vol. 50, p. 135, February 1962.
23. McMurthy, B. J., and A. E. Siegman, *Applied Optics*, Vol. 1, p. 51, January 1962.
24. Bass, M., et al., *Physical Review Letters*, Vol. 8, p. 18, January 1962.
25. Giordmaine, J. A., *Physical Review Letters*, Vol. 8, p. 19, January 1962.
26. Wells, W. H., *Journal of Applied Physics*, Vol. 33, p. 1851, May 1962.
27. Kaminow, I. P., *Physical Review Letters*, Vol. 6, p. 528, May 1962.
28. Eaglesfield, C. C., "Optical Pipeline: A Tentative Assessment," *The Proceedings of the IEE* (British), Vol. 109, Part 8, No. 43, pp. 26–32, January 1962.
29. Fellgett, P., "Theoretical and Practical Explorations of the Use of Television Techniques in Astronomy," *Astronomical Optics and Related Subjects*, Chap. 2, ed. by Zdenek Kopal, North-Holland Publishing Company, Amsterdam, 1956.
30. Oliver, B. M., *Proceedings of the IRE*, Vol. 49, p. 1960, December 1961.
31. Haus, H. A., C. H. Townes, and B. M. Oliver, *Proceedings of the IRE*, Vol. 50, p. 1544, June 1962.
32. Wells, W. H., *Annals of Physics*, Vol. 12, p. 1, January 1961.
33. Strandberg, M., "Inherent Noise of Quantum-Mechanical Amplifiers," *Physical Review*, Vol. 106, No. 4, May 15, 1957.
34. Victor, W. K., R. Stevens, and S. W. Golomb, "Radar Exploration of Venus: Goldstone Observatory Report for March-May, 1961," Technical Report No. 32-132, Jet Propulsion Laboratory, Pasadena, California, August 1, 1962 (also to appear in *IRE Transactions on Space Electronics and Telemetry*, June 1962).
35. Baum, W. A., "The Detection of Faint Images Against the Sky Background," *Transactions at the International Astronomical Union*, Vol. IX, 1957.
36. Allen, C. W., "Astrophysical Quantities," The Athlone Press, London, 1955.
37. Kuiper, G., "The Atmospheres of the Earth and Planets," The University of Chicago Press, Chicago, Ill., 1949.
38. "Kodak Plates and Films for Science and Industry," Eastman Kodak Co., Pamphlet P-9, 1st Ed., 1962.